# High rates of apoptosis visualized in the symbiont-bearing gills of deep-sea *Bathymodiolus* mussels

**Bérénice Piquet[1,2], Bruce Shillito[2], François H. Lallier[1], Sébastien Duperron[2,3,4]\*, Ann C. Andersen[1]\***

**1** Sorbonne Université, CNRS, Lab. Adaptation et Diversité en Milieu Marin, AD2M, Team: Adaptation et Biologie des Invertébrés marins en Conditions Extrêmes (UMR 7144), ABICE, Station Biologique de Roscoff, SBR, Roscoff, France, **2** Sorbonne Université, MNHN, CNRS, IRD, UCN, UA, Lab. Biologie des Organismes et Ecosystèmes Aquatiques BOREA (UMR 7208), Team: Adaptation aux Milieux Extrêmes, AMEX, 7 Quai Saint-Bernard, Paris, France, **3** Muséum National d'Histoire Naturelle, CNRS, Lab. Mécanismes de Communication et Adaptation des Micro-organismes (UMR 7245), Team: Cyanobactéries, Cyanotoxines et Environnement, CCE, 12 rue Buffon, Paris, France, **4** Institut Universitaire de France, Paris, France

\* andersen@sb-roscoff.fr (ACA); sebastien.duperron@mnhn.fr (SD)

## Abstract

Symbiosis between *Bathymodiolus* and Gammaproteobacteria allows these deep-sea mussels to live in toxic environments such as hydrothermal vents and cold seeps. The quantity of endosymbionts within the gill-bacteriocytes appears to vary according to the hosts environment; however, the mechanisms of endosymbiont population size regulation remain obscure. We investigated the possibility of a control of endosymbiont density by apoptosis, a programmed cell death, in three mussel species. Fluorometric TUNEL and active Caspase-3-targeting antibodies were used to visualize and quantify apoptotic cells in mussel gills. To control for potential artefacts due to depressurization upon specimen recovery from the deep-sea, the apoptotic rates between mussels recovered unpressurised, versus mussels recovered in a pressure-maintaining device, were compared in two species from hydrothermal vents on the Mid-Atlantic Ridge: *Bathymodiolus azoricus* and *B. puteoserpentis*. Results show that pressurized recovery had no significant effect on the apoptotic rate in the gill filaments. Apoptotic levels were highest in the ciliated zone and in the circulating hemocytes, compared to the bacteriocyte zone. Apoptotic gill-cells in *B.* aff. *boomerang* from cold seeps off the Gulf of Guinea show similar distribution patterns. Deep-sea symbiotic mussels have much higher rates of apoptosis in their gills than the coastal mussel *Mytilus edulis*, which lacks chemolithoautotrophic symbionts. We discuss how apoptosis might be one of the mechanisms that contribute to the adaptation of deep-sea mussels to toxic environments and/or to symbiosis.

## Introduction

Symbiosis is of major significance to life on Earth. Because symbiosis between two (or several) partners may straddle the line between cooperation and conflict, each partner theoretically initiates and carries on a continued dialogue with the other partners, to keep some degree of control over the interaction. Many symbioses involve partners from different domains of life, such as a eukaryotic host and a bacterial symbiont. The question then arises: how can reciprocal control occur between such distantly related organisms, and are some of the mechanisms involved universal? One of the mechanisms by which an animal host can control symbiont populations is apoptosis. Apoptosis is a programmed cell death involving three main steps: (1) nuclear condensation and fragmentation, (2) cell-wall budding into apoptotic bodies, and (3) their release and possible phagocytosis by neighboring cells [1,2]. Apoptosis plays multiple roles in normal cell turnover, during development, and in the immune system [3].

Its role in symbiosis has also been documented in the cereal weevil *Sitophilus* for example, apoptosis plays a role in regulating the densities of the endosymbiotic bacterium *Sodalis pierantonius*. The symbiont provides essential amino acids that allow the host to rapidly build its protective exoskeleton. Endosymbionts multiply in young adults, but once the cuticle is built, the symbionts are rapidly eliminated through apoptosis of the host cells that contain them [4]. In corals, bleaching occurs in response to heat stress, when the host releases dinoflagellate symbionts through a balance of apoptosis and autophagy: when apoptosis is inhibited, autophagy is initiated as a back-up mechanism, and vice-versa [5]. In addition, apoptosis might act as a post-phagocytic winnowing mechanism in the symbiotic system [6].

At deep-sea hydrothermal vents and cold seeps, the animals that dominate in terms of biomass live in association with chemosynthetic bacteria, which sustain most of their nutrition [7–10]. However, the role apoptosis could play in regulating such symbioses has barely been explored. In the vestimentiferan tubeworms *Riftia pachyptila*, living at vents, and *Lamellibrachia luymesi* from cold seeps, the sulfur-oxidizing symbionts are located within cells of the trophosome. These cells differentiate and proliferate from the trophosome lobule center, then migrate towards the periphery of the lobule where they undergo apoptosis [11]. Ultrastructural observations of the periphery of trophosome lobules show that the symbionts are digested in vacuoles leading to extensive myelin bodies, after which remnants of symbionts disappear while apoptotic nuclei with clumped chromatin patches appear [11]. Thus, in *Riftia* as in the weevil, apoptosis appears to be involved in the process of symbiont regulation and could help the host recover the metabolic investment from the symbiotic phase.

Deep-sea mussels house very dense populations of endosymbionts inside specialized gill epithelial cells, the bacteriocytes [12,13]. In fact, *Bathymodiolus* may constitute by far the densest microbial habitats, in both vents and seeps, although they usually host a very limited diversity of symbiont lineages [7,8]. The relevance to the topic of symbiont control lies in the fact that the association is particularly flexible, with abundances of their symbionts (sulfur- and/or methane-oxidizers) that can change within hours depending on the availability of symbiont substrates in the surrounding water [7,8,14–18]. The symbionts also disappear rapidly if their substrates are absent [17–19]. Ultrastructural studies of the *Bathymodiolus* gill cells have pointed to intracellular digestion of the symbionts within lysosomes as an important carbon transfer mechanism [20–22] suggesting that the host can access the energy stored in its symbionts by killing and digesting them (i.e. a process compared to "farming"). Enzymatic studies involving the detection of acid phosphatases have concluded that some energy from the symbionts can also be transferred to the host through molecules leaking from live symbionts (i.e. a process compared to "milking") [23]. Recent results from whole-gill tissue transcriptomic analyses in the vent species *Bathymodiolus thermophilus* indicated that high symbiont loads

are correlated with under-expression of the genes inhibiting apoptosis, suggesting that when the symbionts are abundant, apoptosis might be activated [24,25]. It can thus be hypothesized that apoptosis is a mechanism by which the hosts control the number of symbionts inside their gills, and possibly obtain their carbon. High throughput sequencing and transcriptomic analyses have shown the great importance of the apoptotic signaling pathways in the gill tissue of several species of *Bathymodiolus* [26–28].

Apoptosis in mollusks is generally triggered by the interaction between immune cells and parasites or pathogens [29]. The high degree of evolutionary conservation of biochemical signaling and executing pathways of apoptosis indicates that programmed cell death likely plays a crucial role in homeostasis and functioning of the molluscan immune system [29–31]. Apoptosis is particularly complex in mollusks, yet the process involves the universal key molecules, named caspases, which are activated in the two major apoptotic pathways: the extrinsic or death receptor pathway, and the intrinsic or mitochondrial pathway [31].The executioner caspase-3 activates a heterodimer protein, the DNA fragmentation factor that is responsible for performing DNA fragmentation [31]. However alternative caspase-independent apoptosis pathways have also been evidenced in mollusks, and cross-talk between different pathways might also be involved [30,31]. Apoptosis was shown to be induced in *Bathymodiolus azoricus* in response to *Vibrio diabolicus* exposure [32]. However the immune gene responses in *B. azoricus* appeared tied to the presence of endosymbiont bacteria, as the progressive weakening of its host transcriptional activity associated with immunity correlates with the gradual disappearance of endosymbiont bacteria from the gill tissues during the extended acclimatization in the sulfide and methane-free aquaria [32]. Thus, the presence of symbionts might modulate the apoptotic patterns in deep-sea symbiotic mussels compared to their coastal mussel relatives without chemolithoautotrophic symbionts.

While several studies have highlighted an important activity of apoptotic signaling factors in three species of *Bathymodiolus (B. azoricus*, *B. manusensis* from hydrothermal vents, and *B. platifrons* from cold seeps [26–28], transcriptomic studies do not give a visual account of this apoptotic activity within the tissues. The present study is the first microscopic investigation of the general distribution patterns of apoptotic cells in the gills, and the first attempt to quantify apoptosis in the different gill cell types of *Bathymodiolus*. We chose to focus on three species, namely *Bathymodiolus azoricus*, *B. puteoserpentis* and *B*. aff. *boomerang*. The first two often dominate the macrofauna at Mid-Atlantic Ridge (MAR) hydrothermal vent sites [33,34]. The third occurs at cold seeps located on the continental margin in the Gulf of Guinea [35]. The former two species are phylogenetically sister species and are also closely related to *B. boomerang* [12]. All three species harbor methane- and sulfur-oxidizing bacteria that co-exist within host cells. Their gills comprise several cell types: epidermal ciliated cells and mucous goblet cells, bacteriocytes hosting the symbionts, interspaced by intercalary cells, and finally circulating hemocytes [36]. Our aim was to investigate whether apoptosis might contribute to regulating symbiont densities. We thus tested whether apoptosis preferentially occurs in bacteriocytes, in particular the most densely populated ones.

As the recovery of deep-sea specimens from several thousand meters depth usually involves a depressurization stress that might alter gene expression and disturb the cell machinery, leading to artefacts [37,38] we performed a comparative analysis of apoptosis in specimens recovered with and without depressurization upon collection. Specimens of *B. azoricus* and *B. puteoserpentis* were recovered using a hyperbaric chamber (PERISCOP—Projet d'Enceinte de Remontée Isobare Servant la Capture d'Organismes Profonds) that allows maintaining their native pressure and temperature throughout recovery [39]. Control specimens recovered without PERISCOP were included. The cold seep *B*. aff. *boomerang* was analyzed to identify potential seep versus vent habitat-related differences, and *Mytilus edulis* was used as a non-

chemolithoautotrophic-symbiont-bearing control mussel. Apoptosis was visualized in gill tissue sections by the TUNEL method (Transferase dUTP Nick-End Labeling) [11,40,41], a common and standard way of visualizing the fragmented DNA in the nucleus of cells undergoing apoptosis. To provide further support for apoptosis, we performed immunolocalization of active Caspase-3, a form of this enzyme that is the overall convergent node of molecular cascades leading to irreversible apoptosis in mollusks [31]. Altogether, this study provides to our knowledge the first visual overview of apoptosis in relation to symbiosis in mussels that host chemosynthetic bacteria.

## Materials and methods

### Specimen collection

This analysis was conducted on 40 individuals of *Bathymodiolus* (Bivalvia, Mytilidae) consisting of 21 *Bathymodiolus azoricus*, ten *B. puteoserpentis* from hydrothermal vents, and nine *B.* aff. *boomerang* from cold seeps. Specimens of *B. azoricus* were collected during the BioBaz 2013 cruise on the Mid-Atlantic Ridge [42]: ten specimens were sampled from the vent fields of Menez Gwen (MG2 marker: 37°50.669N; 31°31.156W, 830 m depth) and eleven specimens from Rainbow site (France 5 marker: 37°17.349N; 32°16.536W, at 2270 m depth). *B. puteoserpentis* were sampled during the BICOSE 2014 cruise [43]. All ten specimens were sampled on the vent site Snake Pit, close to the "Elan" marker (23°22′54″N, 44°55′48″W, at 3520 m depth). For these two species, specimens were recovered either in a standard (i.e. unpressurized) way, or using the PERISCOP hyperbaric vessel (i. e. pressurized samples). The standard collection was done in a waterproof sealed box (BIOBOX) containing local deep-sea water, in which the mussels were exposed to a depressurization corresponding to the depth of their habitat during recovery (approx. 0.1 MPa every 10 m). The pressurized recovery was performed using a small device named the "Croco" sampling cell [44], which was transferred into the PERISCOP pressure-maintaining device [39]. PERISCOP was released from the seafloor through a shuttle system, and surfaced within 45 to 100 minutes, depending on the depth of the mussel habitat. Pressure was monitored during ascent with an autonomous pressure sensor (SP2T4000, NKE Instruments, France). To compare apoptosis between vent and seep mussels, we collected nine specimens of *Bathymodiolus* aff. *boomerang* in a standard manner from the Régab pockmark site in the Gulf of Guinea (M1 marker 5°47.89S, 9°42.62E, 3150 m depth and M2 marker 5°47.85S, 9°42.67E, 3150 m depth) during the 2011 cruise WACS [45]. All three cruises were aboard the RV *Pourquoi Pas*? using the ROV *Victor 6000*. In addition to deep-sea mussels, nine coastal mussels (*Mytilus edulis*) in two sets were analyzed. The first set consisted of wild *M. edulis* collected on rocks from the intertidal seashore in front of Roscoff Marine Station in January 2014 (n = 4 individuals analyzed). The second set of *M. edulis* were cultivated mussels bought from the fishmongers in Paris in January 2017 (n = 5 individuals analyzed). No specific permissions were required for the sampled locations, and the study did not involve endangered or protected species. All data concerning the specimens (recovery, shell measurements and apoptosis percentages) are shown in the S1 Table.

### Sample fixation, inclusion and FISH experiments

Mussel gills were dissected and fixed at 4°C, within 10 minutes after recovery (releasing pressure of the PERISCOP in the case of isobaric recoveries). This short time prevents the risk that apoptotic processes come into play before fixation. Maximum shell length, height under the umbo, and width of the closed shell were measured with a caliper (S1 Fig). Anterior gill fragments were fixed in 4% formaldehyde in sterile-filtered seawater (SFS) for 2 hours. The anterior gill is the oldest part of the gill opposed to the posterior gill containing the budding zone.

Gills were then rinsed in SFS, and dehydrated in increasing series of ethanol (50, 70 and 80%, 15 min each). In the laboratory, gills were embedded in polyethylene glycol (PEG) distearate: 1-hexadecanol (9:1), cut into 8 μm-thick sections using a microtome (Thermo, Germany), recovered on SuperFrost Plus slides (VWR International, USA), and stored at -20°C. Fluorescence *in situ* hybridization (FISH) experiments were performed on some samples to confirm the localization of symbionts following the protocol described previously [7,8,14,15] using probes ImedM-138 (5'-ACCAGGTTGTCCCCCACTAA-3'), specific for methanotrophic symbionts, and probe BangT-642 (5'- CCTATACTCTAGCTTGCCAG-3') specific for sulfur-oxidizing symbionts, and a 30% formamide-containing hybridization buffer.

The gill lamellae were sectioned transversally, to visualize the frontal-abfrontal length of individual filaments. Anatomically in the gill's live position, the frontal sides of the W-shaped gill correspond to the outside surface of the W-branches facing the water currents of the mantle cavity, while the abfrontal sides correspond to the inside of the W-branches, i.e. facing either of the two narrow V-shaped spaces of the W. (S2 Fig).

## TUNEL (Transferase dUTP Nick-End Labeling)

For the detection and quantification of apoptosis, we used the TUNEL method with the *in-situ* cell death detection kit following the manufacturer's instructions (ROCHE, Germany). All slides were first dewaxed then rehydrated by immersion in decreasing series of ethanol. Tissues were rinsed with 1X PBS and permeabilized by proteinase K (20μg.ml$^{-1}$) to enable the binding of dUTP. For permeabilization, various incubation times were tested, and 8 min gave the best results. Slides were then incubated at 37°C for 1h30 with fluorophore dUTP and the enzyme rTdT. Slides were rinsed in three PBS baths (10 min each) to remove the unfixed fluorescein-12-dUTP. In a last step, DNA of all nuclei was labelled with 4'6'-Diamidino-2-phenylindole (DAPI) that is incorporated in the SlowFade Gold Antifade Mounting reagent (Invitrogen, USA). For each analyzed individual, positive and negative controls were performed on adjacent serial sections. The positive control involved a pre-incubation with DNase I (3U/ml, 10 min) before running the full protocol. It produces artificial fragmentation of DNA and exposes 3'OH ends, which bind the green fluorochrome and leads to all nuclei being labelled. The negative control follows the standard protocol but omitting the rTdT enzyme. It reveals autofluorescence of the tissues and possible unspecific fixation of the fluorophore.

## Immunolocalization of active Caspase-3

Slides were dewaxed and rehydrated as for the TUNEL experiments. They were then covered in blocking solution (10X PBS, 2% BSA, 0.3% triton) for 2 h at 4°C. Tissue sections were incubated with the rabbit polyclonal active anti-Caspase-3 primary antibody (directed against a peptide from the P17 fragment of the activated human/mouse Caspase-3) (R&D system, USA). This primary incubation lasted 2 hours at 4°C. Slides were rinsed in 10X PBS three times and covered with the secondary antibody: Alexa Fluor 488-labelled goat anti-rabbit (Invitrogen, dilution 1:500) for 1 h at room temperature. After 3 baths in 10X PBS, slides were mounted with SlowFade. Negative controls were obtained by omitting the primary antibody.

## Image acquisition and analysis

Slides were observed under a BX61 epifluorescence microscope (Olympus, Japan), and pictures were taken under an SP5 confocal (Leica, Germany) at 40X magnification. This magnification enabled a clear resolution for counting each individual labelled nucleus. Entire cross-sections of the TUNEL-labelled gill filaments were represented across 3 to 4 pictures (Figs 1 and 2). The exposure time (or gain on the confocal) was standardized and identical for all
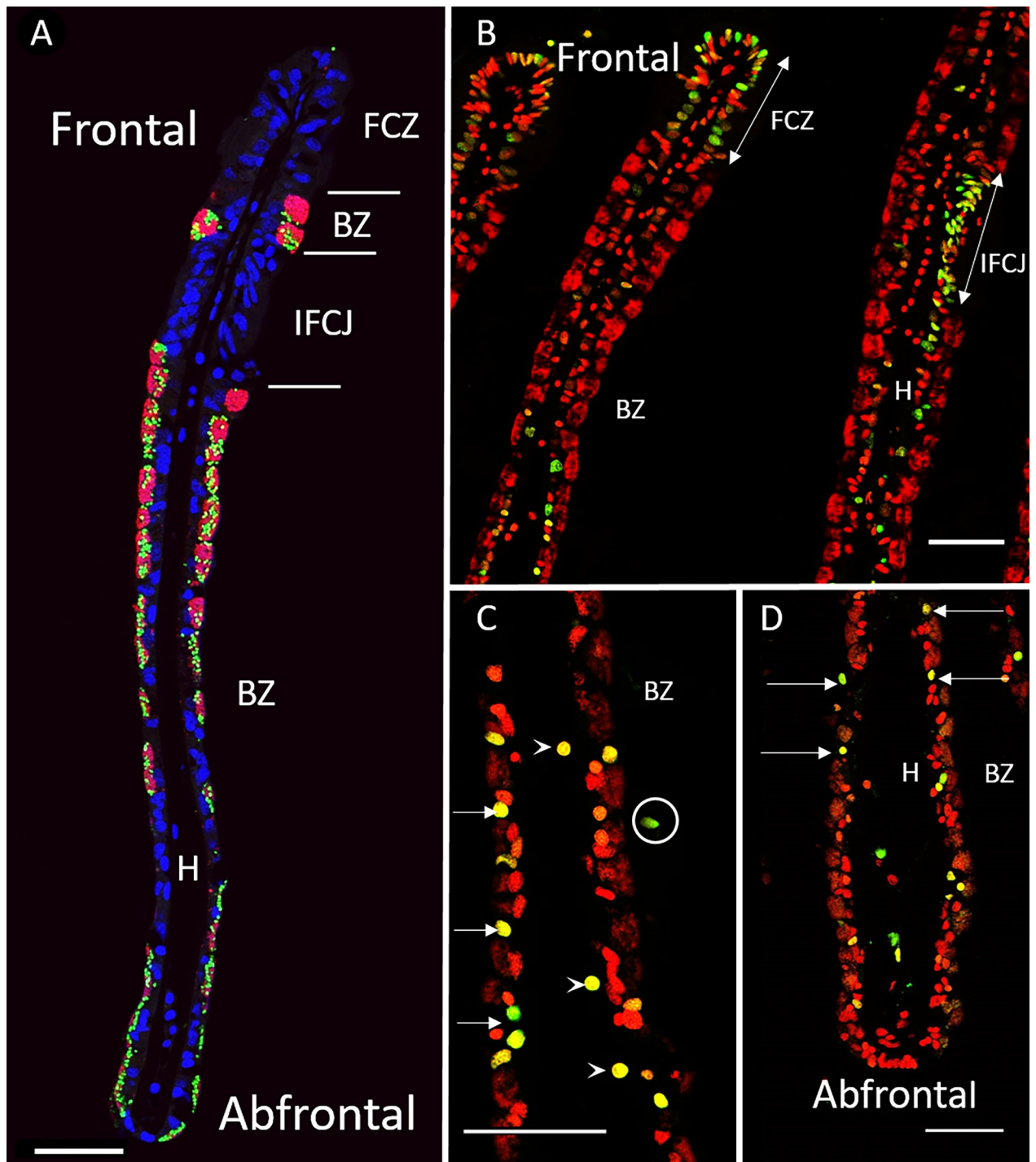
**Fig 1. FISH and TUNEL labelling on gill filaments of *B. azoricus*.** A: Transverse section of gill filaments with FISH labelling. Nuclei from host tissue in blue (DAPI); sulfur-oxidizing symbionts in pink, and methane-oxidizers in green. B, C and D TUNEL-labelled nuclei in green, DAPI staining in red. Arrows point to apoptotic nuclei. B: Ciliated zones often contain many labelled nuclei. C: Bacteriocyte zone that displays many apoptotic nuclei (arrows), apoptotic hemocytes (arrowheads) and an apoptotic cell detached from the basal lamina (circle). D: Abfrontal zone of the gill filament showing apoptotic nuclei in cells with no symbiont (arrows), and apoptotic cells detached from the basal lamina (circles). Abbreviations: BZ: Bacteriocyte zone; FCZ: Frontal Ciliated Zone; H: Hemolymph zone; IFCJ Inter-Filamentary Ciliated Junction. Scale bars: 50μm.

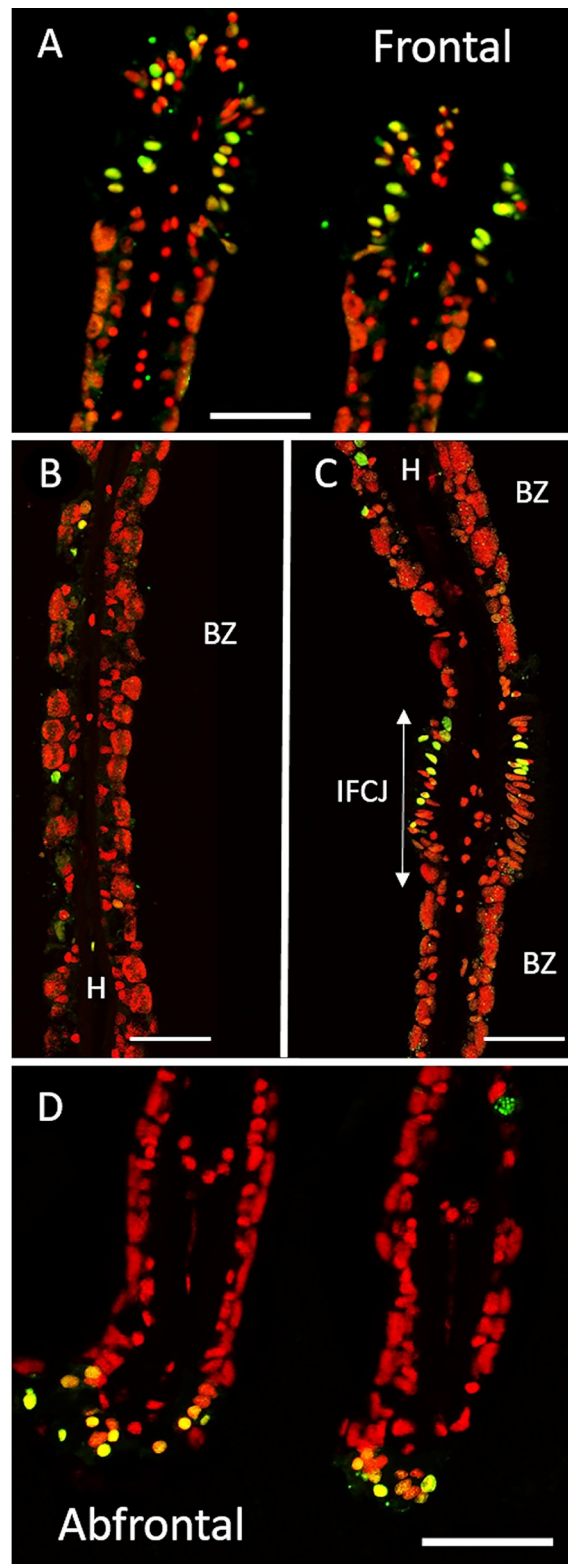https://doi.org/10.1371/journal.pone.0211499.g001

**Fig 2. TUNEL labelling on gill filaments of *B. puteoserpentis*.** TUNEL-labelled nuclei in green, DAPI staining in red. A: Frontal ciliated zones often contain many labelled nuclei. B: Bacteriocyte zone that displays only a few apoptotic nuclei. C: Inter Filamentary ciliated Junction often contain many labelled nuclei. D: Abfrontal zone of the gill filament with apoptotic nuclei. Abbreviations: BZ: Bacteriocyte zone; FCZ: Frontal Ciliated Zone; H: Hemolymph zone; IFCJ Inter-Filamentary Ciliated Junction. Scale bars: 50μm.

https://doi.org/10.1371/journal.pone.0211499.g002

pictures. The 3D-acquisitions were obtained by acquiring images every 0.5 μm throughout the thickness of the section. Slides were observed at 505 nm and 555 nm wavelengths (TUNEL and Caspase 3 signals, respectively), and 400 nm (DAPI). Classical immuno-localization is shown with all labeling in their original color (DAPI in blue), but for TUNEL-labelled nuclei we had to change the DAPI color to red, because blue DNA-labelling overlaid by green (i.e. apoptosis TUNEL labeling) leads to a complex mixture of various levels of green and blue, often making quantitative interpretations difficult. To enable an easy quantitative analysis of the TUNEL images, we chose to set DAPI color to red, so that a double labelling would lead to a third distinct color (yellowish or orange). As TUNEL labels the free 3'OH fragments, we assume that the strongly labelled nuclei showed a higher amount of DNA fragments compared to the weakly stained ones. Since apoptosis is a progressive process occurring within a few hours, we also hypothesize that the bright green nuclei were in a more advanced apoptotic state, than the yellow ones, which in turn are in a more advanced state than the orange-labelled nuclei (i.e. the red DAPI staining is more visible in the orange nuclei that contain very little fragmented DNA). At first, we counted green and yellowish nuclei separately, but as both expressed apoptosis, and early and advanced states were randomly distributed in the gill lamellae (Figs 1 and 2), we pooled them together.

Images were analyzed by counting the labelled nuclei using the free Image J software [46]. Care was taken to count separately each respective cell-type: hemocytes, ciliated cells and finally bacteriocytes and intercalary cells (the latter two being close neighboring cell types, hard to distinguish under the fluorescence microscope, were counted together) (Figs 1 and 2). Thus, for each image, percentages of TUNEL-labelled nuclei were obtained from the hemolymph zone (HZ), the ciliated zone (CZ), and the bacteriocyte zone (BZ) by calculating the ratio between the number of TUNEL-labelled nuclei and the number of DAPI-labeled nuclei present in each respective zone. The ranges of apoptotic percentages counted for each individual are shown zone by zone, and illustrated as boxplots in the S3 Fig. The median percentages for each individual are given in S1 Table.

### Comparisons between species, zones and treatments

The percentage of TUNEL nuclei labelled was used for all analyses after an Arcsine transformation [47].The normality of datasets was tested (Shapiro-Wilk test), which revealed a non-normal distribution of the data. Non-parametric tests were thus applied for inter-groups comparisons (Mann–Whitney–Wilcoxon and Kruskal–Wallis) with the Bonferroni correction for multiple comparisons. All statistical analyses and graph preparation were performed using R (R Development Core Team, version 3.3.3).

## Results

All analyses were performed on transversal sections of the gill lamellae (S2 Fig). From the FISH results, it is noteworthy that bacteriocytes close to the frontal ciliated zone contained large quantities of endosymbionts, and that both the height of the bacteriocytes and their symbiont density decreased towards the abfrontal zone in *B. puteoserpentis*, and *B. azoricus* (Fig 1). This frontal/abfrontal decrease in symbiont density also appears with the DAPI staining, as this labels not only the host nuclei, but also the DNA of the bacterial symbionts.

### Visualization of apoptosis in *Bathymodiolus*

The distribution of TUNEL positive cells in *B. azoricus* and *B. puteoserpentis* is shown in Figs 1 and 2, respectively. In negative controls (S4 Fig), no fluorescence was observed in contrast to positive controls (S4 Fig), except for a bright auto-fluorescence signal seen in clustered round
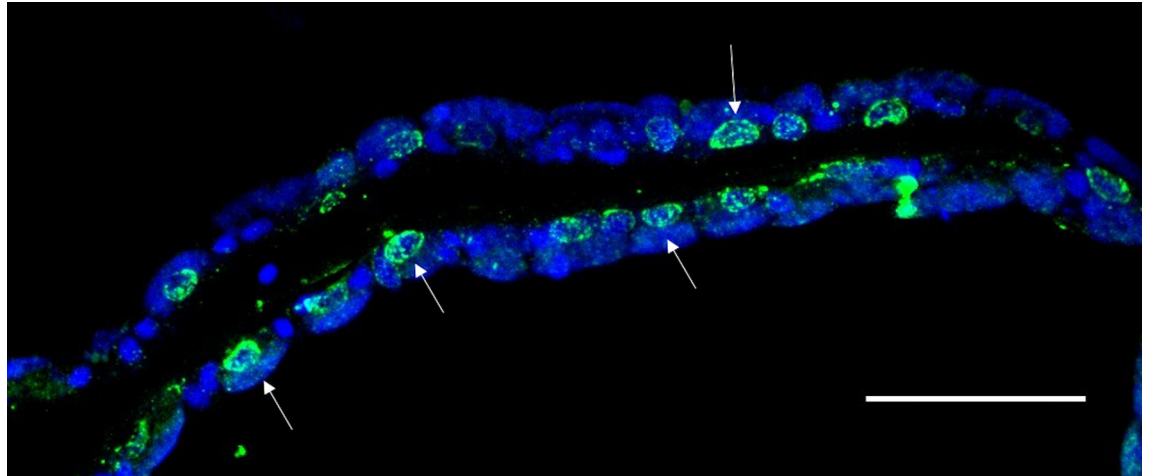
**Fig 3. Active Caspase-3 labelling in the gill of *B. azoricus*.** Typical labelling in green surrounds the nucleus (arrows). DAPI signal in blue. Scale bar: 50μm.

granules. These granules are thought to correspond to mucus droplets present in goblet-cells interspersed among the ciliated cells and along the epithelium of the gill filaments. This auto-fluorescence signal was easy to distinguish from TUNEL signal, as the latter was typically much smaller and brighter.

Nuclei labelled in the TUNEL experiments appears more or less bright leading to bright green, yellow and orange colors, for respectively strong, medium and low amounts of frag-mented DNA (see material and methods for more details). Since apoptosis is a progressive process occurring within a few hours, we hypothesize that the different signal intensities corre-spond to different states of apoptosis advancement, and TUNEL-labelled nuclei were thus counted together to estimate the percentage of apoptotic nuclei in the different regions of the gill lamellae (ciliated zone, bacteriocyte zone and hemolymph) (Figs 1 and 2).

The ciliated frontal zone often is the brightest labelled zone with many strongly labelled cells: up to one cell out of two in some filaments (Figs 1 and 2) giving a clustered appearance of the apo-ptotic cells in the frontal ciliated zone. However, the closest neighbor filament may sometimes only have a few or no labelled cells at all, indicating a great spatial variability in the gill tissue.

Hemocytes were present on all images, but in varying numbers. Many hemocytes are visible on Fig 1C for example, compared to Fig 1B, but more of them were labelled in the latter. TUNEL-labelling in the bacteriocyte zone was heterogeneous: very few nuclei were labelled close to the frontal ciliated zone (Figs 1 and 2), and then increasingly more were labelled when reaching the abfrontal zone (Figs 1 and 2). In the bacteriocyte zone of the abfrontal area, the cells were most of the time devoid of bacteria (Figs 1 and 2).

Active Caspase 3 immunohistochemistry assays yielded strong signals within the cytoplasm of cells, and particularly concentrated around the nuclei (Fig 3). On serial sections within the same individual, the distribution patterns of active Caspase-3 were similar to the TUNEL sig-nal observed, confirming that TUNEL actually revealed apoptotic cells. In general, the active Caspase-3 antibody seemed to label more nuclei than TUNEL.

## Patterns of apoptosis in *Bathymodiolus azoricus* and *B. puteoserpentis*

In total, 31 individuals from the two species were analyzed, representing a total of 19,612 DAPI-labelled nuclei counted on 206 images. The specimens came from deep-sea sites located

at different depths, namely Menez Gwen (-830 m), Rainbow (-2270 m) and Snake Pit (-3520 m). Sampled specimens were either recovered unpressurised (non-isobaric) or with a pressurized (isobaric) recovery. In the latter, PERISCOP reached the surface while retaining 83.6, 76.5 and 70.4% of the native deep-sea pressure at the Menez Gwen, Rainbow and Snake Pit sites, respectively.

First, comparing the global counts in gills of all individuals from all three sites, we noted that there is a great variation in the percentage of apoptotic nuclei among individuals (S3 Fig). This strong heterogeneity indicates that results of statistical analyses must be treated with caution.

In the ciliated (CZ) and bacteriocyte zones (BZ), the percentage of TUNEL-labelled nuclei was not significantly different between the different sites and recovery types (CZ: Kruskal-Wallis test, W = 6.07, df = 5, p-value = 0.30; BZ: Kruskal-Wallis test, W = 3.69, df = 5, p-value = 0.60) (Fig 4 for BZ and S5 Fig for CZ). Similarly, the hemolymph zone showed no significant difference among sites and recovery types (HZ: Kruskal-Wallis test, W = 10.74, df = 5, p-value = 0.05678) (S5 Fig). These results confirm the visual patterns and intensities of TUNEL-labelling in gill filaments of mussels that did not reveal any self-evident difference between specimens from the three sites in either recovery type.

Comparing the global counts (all zones) in gills of all individuals from all three sites, we noted that the greatest level of variation in percentages of apoptotic nuclei occurs among individuals, whatever the site and recovery type (S3 Fig).

For all specimens put together, quantifications indicated median values of 41.3% ($\pm$27%) and 34.5% ($\pm$31%) labelled nuclei in the ciliated and hemolymph zones, respectively. In comparison, the bacteriocyte zone displayed only 19.3% ($\pm$24%) of nuclei that were labelled, (Fig 5) which is significantly less than in the other two cell zones (Kruskal-Wallis test, W = 27.639, df = 2, p-value<0.001, post-hoc test with Bonferroni correction between HZ and BZ, p-value = 0.0002; between CZ and BZ, p-value <0.0001).

### Patterns of apoptosis in the seep species *Bathymodiolus* aff. *boomerang*

TUNEL labelling was applied to the gill filaments of 9 *Bathymodiolus* aff. *boomerang*, based on 40 pictures representing 3,424 nuclei) (Fig 6). Percentages were significantly different among zones (Kruskal-Wallis test, W = 25.00, df = 2, p-value<0.0001). As in the two vent-species studied, apoptosis was more frequent in the ciliated zone (median: 36%, $\pm$23%) and then in the hemocytes (median: 21% $\pm$9%), compared to the bacteriocyte zone (median: 9% $\pm$23%). Overall these results suggest similar patterns in Mytilidae from hydrothermal vents and cold seeps (Fig 7).

Visually, the density of bacteria inside bacteriocytes seems to be more constant between bacteriocytes located in the frontal and in the abfrontal distal edges in *B*. aff. *boomerang* compared to the two vent mussels.

### Patterns of apoptosis in the gill of coastal *Mytilus edulis*

Gill tissues of *Mytilus edulis* were labelled by the TUNEL method (9 specimens from two different localizations, 28 images, 4,091 nuclei). The wild mussels collected on the intertidal rocks near the marine station in January and the commercial mussels bought in Paris in January, have both been collected and fixed after a period of emersion, which is a natural context for intertidal mussels, and both showed the same distribution pattern of apoptotic cells. The number of labelled nuclei was very low in comparison to vent and seep mussels (Fig 6) (median: 1.6%, $\pm$1.6%) with nearly the same percentage across images. In *M. edulis*, the majority of
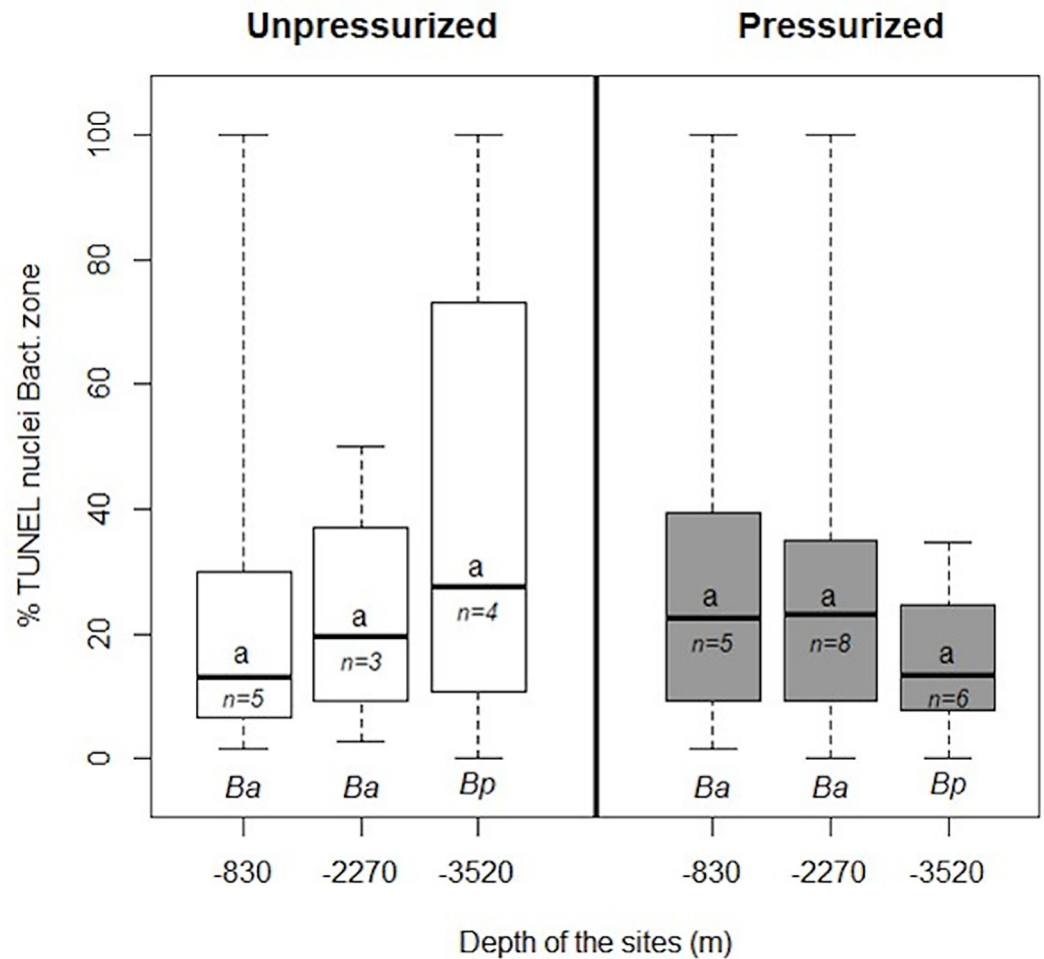
**Unpressurized** **Pressurized**



**Fig 4. Percentages of apoptotic nuclei in the bacteriocyte zone of *B. azoricus* (Ba) and *B. puteoserpentis* (Bp) from the three sites.** White-colored boxplots indicate specimens collected non-isobarically, and grey boxplots indicate those collected isobarically, respectively. Percentages were not significantly different (a, see materials and methods). The letter *n* indicates the number of individuals analyzed for each species. Boxplot whiskers correspond to minimal and maximal values on a single image, the line inside the box is the median, and the upper and lower frames of the boxes represent the first and third quartile respectively.

https://doi.org/10.1371/journal.pone.0211499.g004

labelled nuclei were hemocytes (median: 6.9%, ±10.9%) compared to the epidermal cells (median: 0.9%, ±1.4%).

## Discussion

### Relevance of TUNEL labelling to the study of apoptosis in deep-sea mussels

During apoptosis, DNA undergoes fragmentation, and the TUNEL assay labels the free 3'OH ends that are generated. However, other mechanisms can also lead to DNA fragmentation and would result in a positive TUNEL labelling, and for this reason the TUNEL methodology has been criticized [48–50]. It is nevertheless a standard procedure that has already been applied in mollusk tissues, and in association with active caspase-3 immunolocalization to detect apoptosis in the bivalve *Codakia orbiculata* hosting chemosynthetic symbionts [40,51]. Caspase-3 exists within the cytosol as inactive dimers. All apoptotic pathways in mollusks converge towards a step of cleavage of this zymogen that ultimately results in the triggering of apoptosis
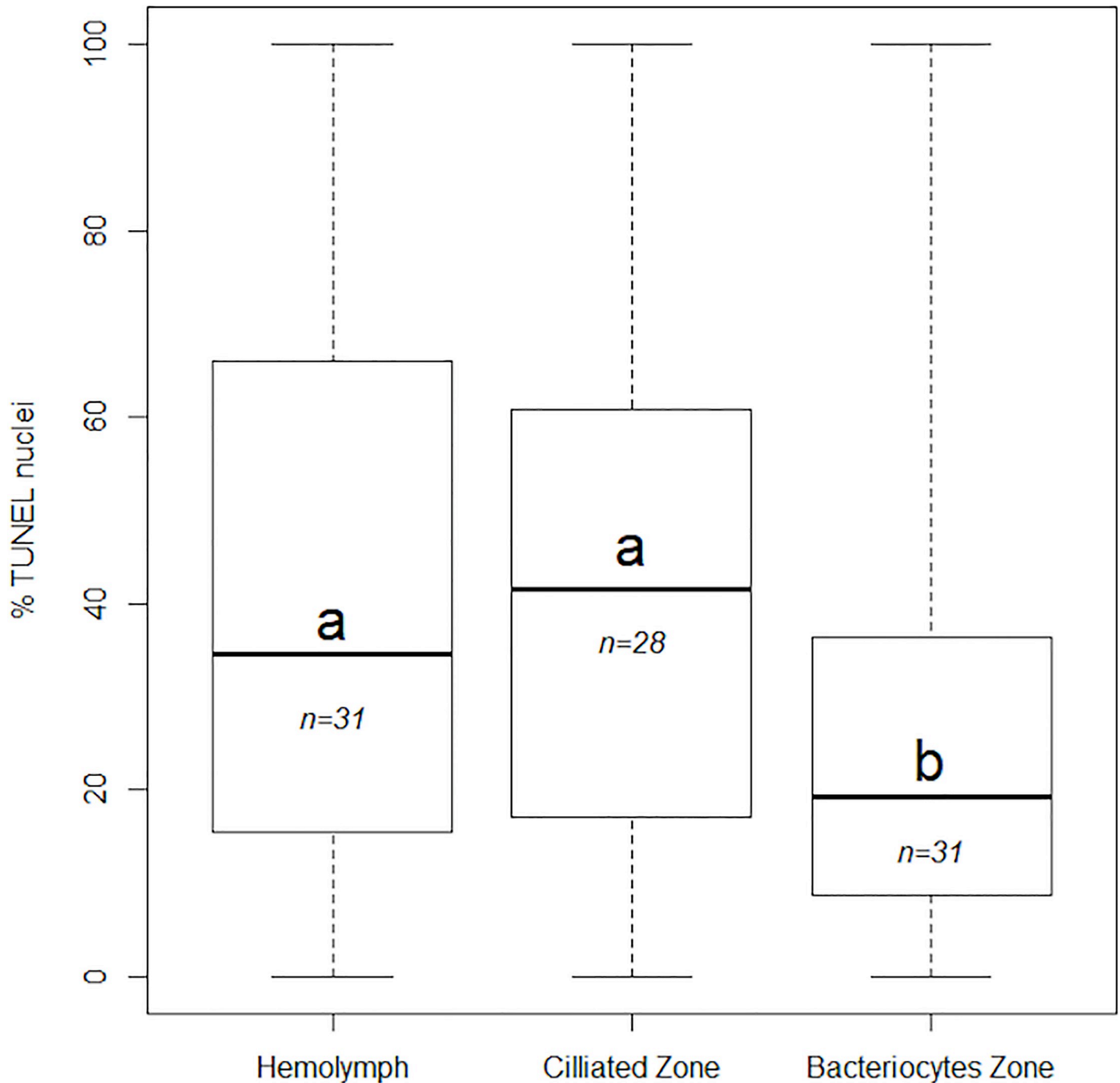
**Fig 5. Percentages of apoptotic nuclei in the hemolymph, ciliated and bacteriocyte zone of _B. azoricus_ and _B. puteoserpentis._** Different letters (a,b) indicate the plots in which median values are statistically different (Wilcoxon test) and n indicates the number of specimens. Boxplot whiskers indicate minimal and maximal values on a single image, the line inside the box is the median, and the upper and lower frames of the boxes represent the first and third quartile respectively.

[31,52]. Although it may have other roles, the activation of Caspase-3 usually leads to cell death by apoptosis. Because other caspases activate necrosis and necroptosis pathways, the occurrence of active Caspase-3 signals rather supports that most observed TUNEL signals actually correspond to apoptotic nuclei [53]. It should however be kept in mind that another
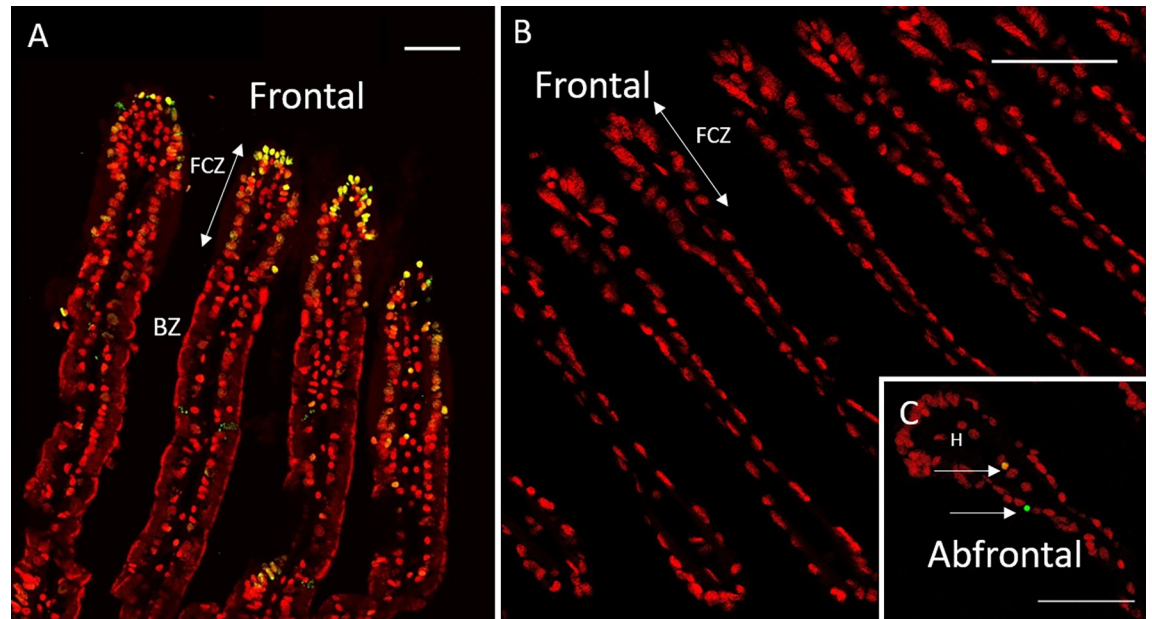
**Fig 6. TUNEL labelling on gill filaments of *Bathymodiolus* aff. *boomerang* (A) and *Mytilus edulis* (B-C).** TUNEL-labelling in green or yellow, DAPI staining in red. A: *Bathymodiolus* aff. *boomerang* displays many labelled nuclei mostly in the frontal ciliated zone. B-C: *Mytilus edulis* gills show very few TUNEL-labelled nuclei, two are visible in the insert (C). Same abbreviations as in Fig 1. Scale bar: 50µm.
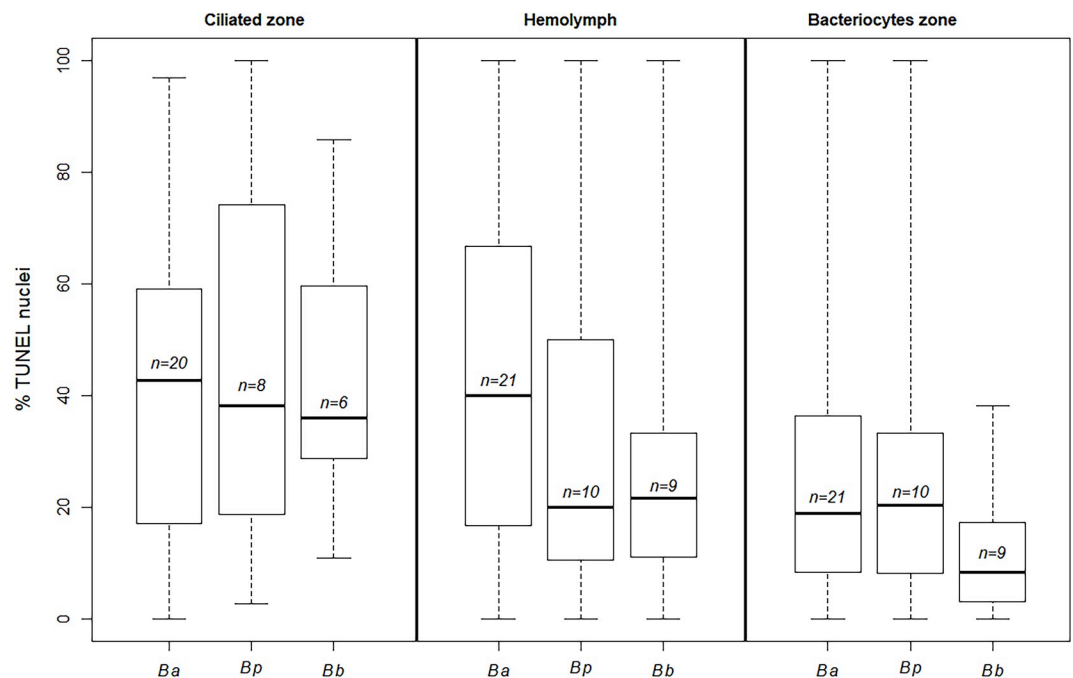
**Fig 7. Percentages of apoptotic nuclei compared between vent and seep species in the ciliated, hemolymph and bacteriocyte zones of *B. azoricus*, *B. puteoserpentis* and *B.* aff. *boomerang* (Ba, Bp and Bb, respectively).** The letter *n* indicates the number of specimens. Boxplot whiskers indicate minimal and maximal values on a single image, line inside the box is the median, and the upper and lower frames of the boxes represent the first and third quartile respectively.

apoptotic pathway exists that is Caspase-independent, as it can take place without activating Caspase-3 [54,55].

## Deep-sea mussels display high rates of apoptosis in their gills

Recovery stress has long been cited as a factor that may prevent accurate assessment of the physiology of deep-sea organisms [39,56,57]. In this study, we found no statistical difference between percentages of apoptotic cells between gills from specimens of *Bathymodiolus azoricus* and *B. puteoserpentis* recovered classically (non-isobaric recovery) and those recovered using the isobaric sampling cell PERISCOP. Thus depressurization during recovery does not seem to trigger massive apoptosis in the gills, although depressurization, by disrupting cells, may alter the distribution of different actors of apoptosis that pass through different cell compartments (mitochondria, nucleus, cell membrane) [39]. No differences were observed between hydrothermal vent sites, regardless of their depth, further suggesting that apoptosis is a natural phenomenon in the gills of deep-sea mussels. Estimates of rates of apoptosis based on TUNEL labelling were much higher in the gills of deep-sea mussels including the seep species *B*. aff. *boomerang*, compared to their coastal relative *Mytilus edulis* lacking chemosynthetic symbionts. This comparison has been made with two different sets of *Mytilus*: wild and cultivated, yielding similarly low percentages and distribution pattern of TUNEL signals. At this stage it is not possible to ascertain whether the much higher levels measured in *Bathymodiolus* are linked with their deep-sea chemosynthetic habitats (for example due to the abundance of xenobiotic compounds and oxidative stressors), with the occurrence of symbionts, or with their different evolutionary history.

## Patterns and potential roles of apoptosis in deep-sea mussels

A major finding in this study is that rates of apoptosis vary considerably among *Bathymodiolus* individual specimens, contrary to *Mytilus*, for a similar investigation effort. This could reveal distinct physiological states among the *Bathymodiolus* at the time of the analysis. Nonetheless, it should be highlighted that apoptosis unfolds rapidly within only a few hours [1]. The distribution of apoptotic cells in a tissue often shows a clustered pattern, as for instance in the mammalian intestine, where apoptotic signal typically appears confined to a cluster of neighboring villi, while other areas of the mucosa appear unstained [41]. A sporadic distribution might ensure a local recycling of the organ, without harming its global function, and might indeed be a characteristic of the apoptotic phenomenon. In the case of *Bathymodiolus*, gills often showed a few TUNEL-positive cells in some cross-sections, and even clusters in the frontal ciliated area of some filaments, but none in the frontal zone of neighboring filaments. This clustered pattern may also contribute to the observed heterogeneity among our individuals. Anyway, the great inter-individual variation prevents us from drawing any definitive conclusion, and results from statistical analysis have to be treated with caution. Nevertheless, there is a clear trend for apoptosis rates to be lower in the bacteriocyte zone than in the ciliated and hemocyte zones.

The very high rates of apoptosis in the ciliated gill cells, in particular compared to *M. edulis*, are intriguing, because these cells do not contain chemolithotrophic symbionts. The gills of *Bathymodiolus* are clearly different from those of the coastal mussels for which, at any given size, the gill surface area is around 20 times smaller [7]. *Bathymodiolus* gills are particularly large and thick, and thus hypertrophied, in relation with the presence of endosymbionts, which might lead to a higher metabolic demand in order to properly deliver water and vital compounds. A great difference between the metabolic demand of symbiotic versus non symbiotic species has indeed been previously evidenced in mussels [58]. These authors have shown

that moderate to high rates of chemoautotrophic or methanotrophic metabolism impose oxygen uptake and proton equivalent elimination demands upon the hosts that are much higher than is typical for their non-symbiotic relatives.

Ciliated cells also display very abundant mitochondria [7,13,59], but this is also the case for *Mytilus edulis*. So, the hypothesis that the great metabolic activity and numerous mitochondria produce large amounts of Reactive Oxygen Species (ROS), resulting in oxidative stress that could lead to increased apoptosis, should then be true in both *Mytilus* and *Bathymodiolus* species [60]. A possible adaptation to meet higher demand in a larger gill would be to increase the turnover rates of the ciliated cells. To achieve this, high rates of cell proliferation could be expected, and this has to be tested. Another hypothesis is linked with fluid toxicity and the direction of water flow in the gills. Ciliated cells are indeed the first to contact the surrounding fluid, and thus exposed to the highest levels of reduced compounds including toxic sulfur and various metals that possibly trigger apoptosis [61]. This may also explain why symbionts tend to be more abundant in the bacteriocytes that are close to the regions that are more exposed to their substrates (mainly methane and sulfide), since these compounds might be more easily accessible to symbionts closer to the frontal zone, sustaining bacterial growth. Cadmium was shown to cause apoptosis on isolated *Crassostrea gigas* hemocytes after 24h *in vitro* incubation in the range of $10–100$ $\mu mol.L^{-1}$ [62]. Gills of mussels are known to accumulate metals, and *Bathymodiolus azoricus* exposed to cadmium display antioxidant enzymatic activities that may be partly due to the endosymbionts [63]. These could contribute to protect bacteriocytes, but not the symbiont-free ciliated cells, resulting in higher apoptosis rates in the latter. *In vivo* incubation experiments at *in situ* pressure would be necessary to test these oxidative stress and fluid toxicity hypotheses.

Apoptosis of circulating and resident hemocytes occurs at a high baseline level in mollusks [29], and we estimated that 34.5% of the hemocytes were apoptotic in *B. azoricus* and *B. puteoserpentis*. The immune system of mussels relies on innate immunity only, and hemocytes are also suspected to play key role in the immune response. Hemocytes are also suspected to have a role in detoxification [59]. In *Crassostrea virginica*, the most common apoptotic cell type is the hemocyte. The apoptotic index for *Crassostrea* hemocytes, calculated the same way as herein, but using another visualization method (Apoptag), ranges between 23 and 99% with a mean of 46% [64]. In another study, *Crassostrea virginica* displayed between 4.5% and 15.3% of apoptotic circulating hemocytes (Annexin-V assay) [65]. These results are congruent with the rates observed in this study and could reveal overall high apoptosis rates in the hemocytes of bivalves, visually confirming the importance of apoptosis in the innate immune system.

Despite the fact that apoptosis rates are high in *Bathymodiolus* bacteriocytes compared to those in *M. edulis* epithelial gill-cells, they are only roughly half of those measured in ciliated cells and hemocytes. Results from transcriptomic studies and their subsequent interpretation by other authors led to the hypothesis that apoptosis was the main mechanism that allowed mussels (initially *Bathymodiolus thermophilus*) to control the amount of symbionts in their gills. The underlying idea was that bacteria-filled bacteriocytes would undergo apoptosis in a way similar to that observed in the tubeworm *Riftia pachyptila*, in which this mechanism participates to the recovery of symbiont carbon, and recycling of the animal cells [11]. However, our observations show that the bacteriocytes that contain only a few, or no bacteria at all, are mainly those that enter into apoptosis. Lower levels of apoptosis in bacteriocytes, predominantly those where symbionts are the most abundant, could be explained by a putative endosymbiont-linked protection against apoptosis-provoking compounds. This could explain why cells with fewer bacteria, mostly located in the distal (i.e. abfrontal) edge away from the ciliated zone and possibly most depleted in symbiont substrates, would preferentially enter apoptosis, although this is merely hypothetical at this stage.

Overall, it appears that high rates of apoptosis are a normal feature in deep-sea mussel gills physiology. Rather than being a direct mechanism used to kill the most bacteria-rich cells in order to gain carbon, apoptosis seems to be involved in the overall dynamics of the gill organ itself. Indeed, observed patterns indicate that the cells harboring few to no bacteria are more often apoptotic. This can be interpreted in the light of gill specialization to symbiosis, with enlarged gills requiring stronger cilia activity, which possibly leads to higher turnover of ciliated cells, and habitat characteristics including the presence of toxic compounds. Apoptosis mechanisms are known to play major roles in other symbioses [4,5,11,66]. For example, *Codakia orbiculata*, a shallow water bivalve that hosts Gammaproteobacteria in its gills can lose and reacquire symbionts. After loss of the symbionts, the bacteriocytes multiply massively to reacquire bacteria, while the bacteriocytes in later colonization stages are eliminated by apoptosis [40]. A similar mechanism may be occurring in mussels. At first, apoptosis could appear as a heavy cost for the host, especially given that it may endanger the whole organ. However, neighboring cells could phagocytose the cells that undergo apoptosis, allowing recycling of their constituents. Apoptotic cells also tend to detach from the basal lamina, and once detached they may be treated as food particles by the mussels, again allowing recycling. The correlation observed in previous transcriptome analyses [25] between apoptotic rates and overall symbiont content may then be indirect: hosts with more bacteria tend to have larger gills [7], and thus more active ciliated cells, so overall more cells in apoptosis. High rates of apoptosis should thus be regarded as an integral part of the adaptation of deep-sea mussels to their symbioses and their habitats, and visualization patterns indicates that apoptosis probably plays more complex roles than previously assumed. This study has only investigated adult specimens, but because mussels acquire their symbionts in their post-larval stage and throughout the host lifetime [67,68], the coupling of symbiont acquisition with apoptosis should be explored at all developmental stages. Further study should also investigate the impact of stress (toxic compounds, temperature) and those of symbiont loss (when *Bathymodiolus* is moved away from the fluids compounds [18,69]) on the rates of apoptosis, as well as cell proliferation patterns. Because of the relative simplicity of the mussel holobiont, its high bacterial load and high levels of apoptosis, deep-sea mussels may prove useful models to further investigate the links between apoptosis, autophagy and symbiosis.

## Supporting information

**S1 Table. Median percentage of apoptosis in all individuals from the four species in this study, with their shell measurements, collection site, and method of recovery.**
(DOCX)

**S1 Fig. Measurements of mussel shells.** Using a caliper, the length, width and thickness of each individual was taken as shown on the figure, and recorded in S1 Table.
(TIF)

**S2 Fig. Gills of *Bathymodiolus* spp.** A: *Bathymodiolus azoricus* with open mantle cavity showing its two gills. The frame corresponds to the anterior gill part used in this study. B: Gills from one side (adapted from [70] showing the unfused W-shaped pairs of demibranchs and the ventral-transversal plane of sectioning across the gill lamellae (orange framed box).
(TIFF)

**S3 Fig.  Percentage of apoptotic nuclei in the ciliated (A), hemolymph (B) and bacteriocyte (C) zones in individual specimens of *B. azoricus* and *B. puteoserpentis* from the three sites.** White and grey boxplots indicate specimens from non-isobaric and isobaric recoveries, respectively. Boxplot whiskers indicate minimal and maximal values of percentage of TUNEL-

labelled nuclei on a single image, the line inside the box is the median, the line inside the box is the median, and the upper and lower frames of the boxes represent the first and third quartile respectively. The bold horizontal line through all boxplots represents the median of all pictures. The numbers below the Y-axis of the figures correspond to the specimen ID.
(TIFF)

**S4 Fig. TUNEL labelling on gill filaments of *Bathymodiolus azoricus*.** A. Positive control with all nuclei labelled (in green). B. Negative control with non-specific autofluorescent putative mucus-like granules (arrow). Scale bars: 50μm.
(TIF)

**S5 Fig. Percentage of apoptotic nuclei in the ciliated (A) and hemolymph zones (B) of *B. azoricus* and *B. puteoserpentis* from the three sites.** Grey and white boxplots indicate specimens from isobaric and non-isobaric recoveries, respectively. No significant differences were seen among groups (Pairwise Wilcoxon with Bonferroni's standard correction). Boxplot whiskers indicate minimal and maximal values on a single image, line inside the box is the median, and the upper and lower frames of the boxes represent the first and third quartiles respectively.
(TIFF)

## Acknowledgments

## Author Contributions

**Conceptualization:** Ann C. Andersen.

**Data curation:** Sébastien Duperron, Ann C. Andersen.

**Formal analysis:** Sébastien Duperron, Ann C. Andersen.

**Funding acquisition:** François H. Lallier, Sébastien Duperron, Ann C. Andersen.

**Investigation:** Bérénice Piquet, Bruce Shillito, François H. Lallier, Sébastien Duperron, Ann C. Andersen.

**Methodology:** Bérénice Piquet, Bruce Shillito, Ann C. Andersen.

**Project administration:** Sébastien Duperron, Ann C. Andersen.

**Resources:** Bruce Shillito, François H. Lallier, Sébastien Duperron.

**Supervision:** Sébastien Duperron, Ann C. Andersen.

**Validation:** Sébastien Duperron, Ann C. Andersen.

**Visualization:** Bérénice Piquet, Ann C. Andersen.

**Writing – original draft:** Bérénice Piquet, Bruce Shillito, François H. Lallier, Sébastien Duperron, Ann C. Andersen.

**Writing – review & editing:** Bérénice Piquet, Sébastien Duperron, Ann C. Andersen.

## References

1. Kerr JFR, Wyllie AH, Currie AR. Apoptosis: a basic biological phenomenon with wide-ranging implications in tissue kinetics. Br J Cancer 1972; 26:239–57. PMID: 4561027

2. Häcker G. The morphology of apoptosis. Cell Tissue Res 2000; 301:5–17. https://doi.org/10.1007/s004410000193 PMID: 10928277

3. Elmore S. Apoptosis: a review of programmed cell death. Toxicol Pathol 2007; 35:495–516. https://doi.org/10.1080/01926230701320337 PMID: 17562483

4. Vigneron A, Masson F, Vallier A, Balmand S, Rey M, Vincent-Monégat C, et al. Insects recycle endosymbionts when the benefit is over. Curr Biol 2014; 24:2267–73. https://doi.org/10.1016/j.cub.2014.07.065 PMID: 25242028

5. Dunn SR, Schnitzler CE, Weis VM. Apoptosis and autophagy as mechanisms of dinoflagellate symbiont release during cnidarian bleaching: every which way you lose. Proc R Soc B Biol Sci 2007; 274:3079–85. https://doi.org/10.1098/rspb.2007.0711 PMID: 17925275

6. Dunn SR, Weis VM. Apoptosis as a post-phagocytic winnowing mechanism in a coral-dinoflagellate mutualism. Environ Microbiol 2009; 11:268–76. https://doi.org/10.1111/j.1462-2920.2008.01774.x PMID: 19125818

7. Duperron S, Quiles A, Szafranski KM, Léger N, Shillito B. Estimating symbiont abundances and gill surface areas in specimens of the hydrothermal vent mussel *Bathymodiolus puteoserpentis* maintained in pressure vessels. Front Mar Sci 2016; 3:1–12. https://doi.org/10.3389/fmars.2016.00016

8. Duperron S. The diversity of deep-sea mussels and their bacterial symbioses. In: Kiel S, editor. Vent Seep Biota, vol. 33, Dordrecht: Springer; 2010, p. 137–67.

9. Fisher CR, Childress JJ, Oremland RS, Bidigare RR. The importance of methane and thiosulfate in the metabolism of the bacterial symbionts of two deep-sea mussels. Mar Biol 1987; 96:59–71. https://doi.org/10.1007/BF00394838

10. Sibuet M, Olu K. Biogeography, biodiversity and fluid dependence of deep-sea cold-seep communities at active and passive margins. Deep Sea Res Part II 1998; 45:517–67. https://doi.org/10.1016/S0967-0645(97)00074-X

11. Pflugfelder B, Cary SC, Bright M. Dynamics of cell proliferation and apoptosis reflect different life strategies in hydrothermal vent and cold seep vestimentiferan tubeworms. Cell Tissue Res 2009; 337:149–65. https://doi.org/10.1007/s00441-009-0811-0 PMID: 19444472

12. Lorion J, Kiel S, Faure B, Kawato M, Ho SYW, Marshall B, et al. Adaptive radiation of chemosymbiotic deep-sea mussels. Proc R Soc B Biol Sci 2013; 280:20131243–20131243. https://doi.org/10.1098/rspb.2013.1243 PMID: 24048154

13. Fiala-Médioni A, Métivier C, Herry A, Le Pennec M. Ultrastructure of the gill of the hydrothermal-vent mytilid *Bathymodiolus sp.* Mar Biol 1986; 92:65–72. https://doi.org/10.1007/BF00392747

14. Szafranski KM, Piquet B, Shillito B, Lallier FH, Duperron S. Relative abundances of methane- and sulfur-oxidizing symbionts in gills of the deep-sea hydrothermal vent mussel *Bathymodiolus azoricus* under pressure. Deep Sea Res Part Oceanogr Res Pap 2015; 101:7–13. https://doi.org/10.1016/j.dsr.2015.03.003

15. Halary S, Riou V, Gaill F, Boudier T, Duperron S. 3D FISH for the quantification of methane- and sulphur-oxidizing endosymbionts in bacteriocytes of the hydrothermal vent mussel *Bathymodiolus azoricus*. ISME J 2008; 2:284–92. https://doi.org/10.1038/ismej.2008.3 PMID: 18219282

16. Riou V, Halary S, Duperron S, Bouillon S, Elskens M, Bettencourt R, et al. Influence of $CH_4$ and $H_2S$ availability on symbiont distribution, carbon assimilation and transfer in the dual symbiotic vent mussel *Bathymodiolus azoricus*. Biogeosciences 2008; 5:1681–91. https://doi.org/10.5194/bg-5-1681-2008

17. Guezi H, Boutet I, Andersen AC, Lallier FH, Tanguy A. Comparative analysis of symbiont ratios and gene expression in natural populations of two *Bathymodiolus* mussel species. Symbiosis 2014; 63:19–29. https://doi.org/10.1007/s13199-014-0284-0

18. Kádár E, Bettencourt R, Costa V, Santos RS, Lobo-da-Cunha A, Dando P. Experimentally induced endosymbiont loss and re-acquirement in the hydrothermal vent bivalve *Bathymodiolus azoricus*. J Exp Mar Biol Ecol 2005; 318:99–110. https://doi.org/10.1016/j.jembe.2004.12.025

19.  Riou V, Colaço A, Bouillon S, Khripounoff A, Dando P, Mangion P, et al. Mixotrophy in the deep sea: a dual endosymbiotic hydrothermal mytilid assimilates dissolved and particulate organic matter. Mar Ecol Prog Ser 2010; 405:187–201. https://doi.org/10.3354/meps08515

20.  Barry JP, Buck KR, Kochevar RK, Nelson DC, Fujiwara Y, Goffredi SK, et al. Methane-based symbiosis in a mussel, *Bathymodiolus platifrons*, from cold seeps in Sagami Bay, Japan. Invertebr Biol 2002; 121:47–54. https://doi.org/10.1111/j.1744-7410.2002.tb00128.x

21.  Fiala-Medioni A, Michalski J-C, Jollès J, Alonso C, Montreuil J. Lysosomic and lysozyme activities in the gill of bivalves from deep hydrothermal vents. Comptes Rendus Académie Sci Paris 1994; 317:239–44.

22.  Streams ME, Fisher CR, Fiala-Medioni A. Methanotrophic symbiont location and fate of carbon incorporated from methane in a hydrocarbon seep mussel. Mar Biol 1997; 129:465–476.

23.  Kádár E, Davis SA, Lobo-da-Cunha A. Cytoenzymatic investigation of intracellular digestion in the symbiont-bearing hydrothermal bivalve *Bathymodiolus azoricus*. Mar Biol 2008; 153:995–1004. https://doi.org/10.1007/s00227-007-0872-0

24.  Boutet I, Ripp R, Lecompte O, Dossat C, Corre E, Tanguy A, et al. Conjugating effects of symbionts and environmental factors on gene expression in deep-sea hydrothermal vent mussels. BMC Genomics 2011; 12:1–13. https://doi.org/10.1186/1471-2164-12-530 PMID: 22034982

25.  Guezi H, Boutet I, Tanguy A, Lallier FH. The potential implication of apoptosis in the control of chemosynthetic symbionts in *Bathymodiolus thermophilus*. Fish Shellfish Immunol 2013; 34:1709. https://doi.org/10.1016/j.fsi.2013.03.223

26.  Bettencourt R, Pinheiro M, Egas C, Gomes P, Afonso M, Shank T, et al. High-throughput sequencing and analysis of the gill tissue transcriptome from the deep-sea hydrothermal vent mussel *Bathymodiolus azoricus*. BMC Genomics 2010; 11:559. https://doi.org/10.1186/1471-2164-11-559 PMID: 20937131

27.  Wong YH, Sun J, He LS, Chen LG, Qiu J-W, Qian P-Y. High-throughput transcriptome sequencing of the cold seep mussel *Bathymodiolus platifrons*. Sci Rep 2015; 5:16597. https://doi.org/10.1038/srep16597 PMID: 26593439

28.  Zheng P, Wang M, Li C, Sun X, Wang X, Sun Y, et al. Insights into deep-sea adaptations and host-symbiont interactions: a comparative transcriptome study on *Bathymodiolus* mussels and their coastal relatives. Mol Ecol 2017:5133–48. https://doi.org/10.1111/mec.14160 PMID: 28437568

29.  Sokolova IM. Apoptosis in molluscan immune defense. Invertebr Surviv J 2009; 6:49–58.

30.  Kiss T. Apoptosis and its functional significance in molluscs. Apoptosis 2010; 15:313–21. https://doi.org/10.1007/s10495-009-0446-3 PMID: 20047074

31.  Romero A, Novoa B, Figueras A. The complexity of apoptotic cell death in mollusks: An update. Fish Shellfish Immunol 2015; 46:79–87. https://doi.org/10.1016/j.fsi.2015.03.038 PMID: 25862972

32.  Barros I, Mendes S, Rosa D, Serrão Santos R, Bettencourt R. *Vibrio diabolicus* immunomodulatory effects on *Bathymodiolus azoricus* during long-term acclimatization at atmospheric pressure. J Aquac Res Dev 2016; 7. https://doi.org/10.4172/2155-9546.1000464

33.  Cosel R von, Métivier B, Hashimoto J. Three new species of *Bathymodiolus* (Bivalvia: Mytilidae) from hydrothermal vents in the Lau Basin and the north Fiji Basin, western Pacific, and the Snake Pit area, Mid-Atlantic Ridge. The Veliger 1994; 37:374–92.

34.  Cosel R von, Comtet T, Krylova EM. *Bathymodiolus* (Bivalvia: Mytilidae) from hydrothermal vents on the Azores Triple Junction and the Logatchev Hydrothermal Field, Mid-Atlantic Ridge. The Veliger 1999; 42:218–48.

35.  Olu-Le Roy K, Cosel R von, Hourdez S, Carney SL, Jollivet D. Amphi-Atlantic cold-seep *Bathymodiolus species* complexes across the equatorial belt. Deep Sea Res Part Oceanogr Res Pap 2007; 54:1890–911. https://doi.org/10.1016/j.dsr.2007.07.004

36.  Fiala-Medioni A, McKiness ZP, Dando PR, Boulegue J, Mariotti A, Alayse A-M, et al. Ultrastructural, biochemical, and immunological characterization of two populations of the mytilid mussel *Bathymodiolus azoricus* from the Mid-Atlantic Ridge: evidence for a dual symbiosis. Mar Biol 2002; 141:1035–43. https://doi.org/10.1007/s00227-002-0903-9

37.  Pradillon F. High hydrostatic pressure environments. In: Bell EM, editor. Life Extrem. Environ. Org. Strateg. Surviv., Wallingford: CABI; 2012, p. 271–95. https://doi.org/10.1079/9781845938147.0271

38.  Pradillon F, Gaill F. Pressure and life: some biological strategies. Rev Environ Sci Biotechnol 2007; 6:181–95. https://doi.org/10.1007/s11157-006-9111-2

39.  Shillito B, Hamel G, Duchi C, Cottin D, Sarrazin J, Sarradin P-M, et al. Live capture of megafauna from 2300m depth, using a newly designed Pressurized Recovery Device. Deep Sea Res Part Oceanogr Res Pap 2008; 55:881–9. https://doi.org/10.1016/j.dsr.2008.03.010

**40.** Elisabeth NH, Gustave SDD, Gros O. Cell proliferation and apoptosis in gill filaments of the lucinid *Codakia orbiculata* (Montagu, 1808) (Mollusca: Bivalvia) during bacterial decolonization and recolonization. Microsc Res Tech 2012; 75:1136–46. https://doi.org/10.1002/jemt.22041 PMID: 22438018

**41.** Gavrieli Y, Sherman Y, Ben-Sasson SA. Identification of programmed cell death *in situ* via specific labeling of nuclear DNA fragmentation. J Cell Biol 1992; 119:493–501. PMID: 1400587

**42.** Lallier F. BIOBAZ 2013 cruise, Pourquoi pas? R/V 2013. https://doi.org/10.17600/13030030

**43.** Cambon-Bonavita M-A. BICOSE cruise, Pourquoi pas? R/V 2014. https://doi.org/10.17600/14000100

**44.** Ravaux J, Hamel G, Zbinden M, Tasiemski AA, Boutet I, Léger N, et al. Thermal limit for metazoan life in question: *In vivo* heat tolerance of the pompeii worm. PLoS ONE 2013; 8:e64074. https://doi.org/10.1371/journal.pone.0064074 PMID: 23734185

**45.** Olu K. WACS cruise, Pourquoi pas? R/V 2011. https://doi.org/10.17600/11030010

**46.** Abràmoff MD, Magalhães PJ, Ram SJ. Image processing with ImageJ. Biophotonics Int 2004; 11:36–42. https://doi.org/10.1016/j.tcb.2004.03.002.

**47.** Duperron S, Guezi H, Gaudron SM, Pop Ristova P, Wenzhöfer F, Boetius A. Relative abundances of methane- and sulphur-oxidising symbionts in the gills of a cold seep mussel and link to their potential energy sources: Variability of symbiont abundances in a seep mussel. Geobiology 2011; 9:481–91. https://doi.org/10.1111/j.1472-4669.2011.00300.x PMID: 21978364

**48.** de Torres C, Munell F, Ferrer I, Reventos J, Macaya A. Identification of necrotic cell death by the TUNEL assay in the hypoxic-ischemic neonatal rat brain. Neurosci Lett 1997; 230:1–4. PMID: 9259449

**49.** Labat-Moleur F, Guillermet C, Lorimier P, Robert C, Lantuejoul S, Brambilla E, et al. TUNEL apoptotic cell detection in tissue sections: critical evaluation and improvement. J Histochem Cytochem 1998; 46:327–34. https://doi.org/10.1177/002215549804600306 PMID: 9487114

**50.** Kroemer G, Galluzzi L, Vandenabeele P, Abrams J, Alnemri ES, Baehrecke EH, et al. Classification of cell death: recommendations of the Nomenclature Committee on Cell Death 2009. Cell Death Differ 2009; 16:3–11. https://doi.org/10.1038/cdd.2008.150 PMID: 18846107

**51.** Motta CM, Frezza V, Simoniello P. Caspase 3 in molluscan tissues: Localization and possible function. J Exp Zool Part Ecol Genet Physiol 2013; 319:548–59. https://doi.org/10.1002/jez.1817 PMID: 24039235

**52.** Boatright KM, Salvesen GS. Mechanisms of caspase activation. Curr Opin Cell Biol 2003; 15:725–31. https://doi.org/10.1016/j.ceb.2003.10.009 PMID: 14644197

**53.** Yuan J, Najafov A, Py BF. Roles of Caspases in Necrotic Cell Death. Cell 2016; 167:1693–704. https://doi.org/10.1016/j.cell.2016.11.047 PMID: 27984721

**54.** Chipuk JE, Green DR. Do inducers of apoptosis trigger caspase-independent cell death? Nat Rev Mol Cell Biol 2005; 6:268–75. https://doi.org/10.1038/nrm2239 PMID: 15714200

**55.** Abraham MC, Shaham S. Death without caspases, caspases without death. Trends Cell Biol 2004; 14:184–93. https://doi.org/10.1016/j.tcb.2004.03.002 PMID: 15066636

**56.** Childress JJ, Barnes AT, Quetin LB, Robison BH. Thermally protecting cod ends for the recovery of living deep-sea animals. Deep Sea Res 1978; 25:419–22. https://doi.org/10.1016/0146-6291(78)90568-4

**57.** Shillito B, Gaill F, Ravaux J. The IPOCAMP pressure incubator for deep-sea fauna. J Mar Sci Technol 2014; 22:97–102. https://doi.org/10.6119/JMST-013-0718-3

**58.** Childress JJ, Girguis PR. The metabolic demands of endosymbiotic chemoautotrophic metabolism on host physiological capacities. J Exp Biol 2011; 214:312–25. https://doi.org/10.1242/jeb.049023 PMID: 21177951

**59.** Fiala-Medioni A. Synthèse sur les adaptations structurales liées à la nutrition des mollusques bivalves des sources hydrothermales profondes. Oceanol Acta 1988;N˚SP:173–9.

**60.** Mone Y, Monnin D, Kremer N. The oxidative environment: a mediator of interspecies communication that drives symbiosis evolution. Proc R Soc B Biol Sci 2014; 281:20133112–20133112. https://doi.org/10.1098/rspb.2013.3112 PMID: 24807248

**61.** Circu ML, Aw TY. Reactive oxygen species, cellular redox systems, and apoptosis. Free Radic Biol Med 2010; 48:749–62. https://doi.org/10.1016/j.freeradbiomed.2009.12.022 PMID: 20045723

**62.** Sokolova IM. Cadmium-induced apoptosis in oyster hemocytes involves disturbance of cellular energy balance but no mitochondrial permeability transition. J Exp Biol 2004; 207:3369–80. https://doi.org/10.1242/jeb.01152 PMID: 15326213

**63.** Company R, Serafim A, Bebianno MJ, Cosson R, Shillito B, Fiala-Médioni A. Effect of cadmium, copper and mercury on antioxidant enzyme activities and lipid peroxidation in the gills of the hydrothermal vent mussel *Bathymodiolus azoricus*. Mar Environ Res 2004; 58:377–81. https://doi.org/10.1016/j.marenvres.2004.03.083 PMID: 15178056

**64.** Sunila I, LaBanca J. Apoptosis in the pathogenesis of infectious diseases of the eastern oyster *Crassostrea virginica*. Dis Aquat Organ 2003; 56:163–70. https://doi.org/10.3354/dao056163 PMID: 14598992

**65.** Goedken M, Morsey B, Sunila I, Dungan C, De Guise S. The effects of temperature and salinity on apoptosis of *Crassostrea virginica* hemocytes and *Perkinsus marinus*. J Shellfish Res 2005; 24:177–83. https://doi.org/10.2983/0730-8000(2005)24[177:TEOTAS]2.0.CO;2

**66.** Foster JS, McFall-Ngai MJ. Induction of apoptosis by cooperative bacteria in the morphogenesis of host epithelial tissues. Dev Genes Evol 1998; 208:295–303. PMID: 9716720

**67.** Wentrup C, Wendeberg A, Huang JY, Borowski C, Dubilier N. Shift from widespread symbiont infection of host tissues to specific colonization of gills in juvenile deep-sea mussels. ISME J 2013; 7:1244–7. https://doi.org/10.1038/ismej.2013.5 PMID: 23389105

**68.** Wentrup C, Wendeberg A, Schimak M, Borowski C, Dubilier N. Forever competent: deep-sea bivalves are colonized by their chemosynthetic symbionts throughout their lifetime: Symbiont colonization in gills of deep-sea bivalves. Environ Microbiol 2014; 16:3699–713. https://doi.org/10.1111/1462-2920.12597 PMID: 25142549

**69.** Raulfs EC, Macko SA, Van Dover CL. Tissue and symbiont condition of mussels (*Bathymodiolus thermophilus*) exposed to varying levels of hydrothermal activity. J Mar Biol Assoc UK 2004; 84:229–34. https://doi.org/10.1017/S0025315404009087h

**70.** Le Pennec M, Hily A. Anatomie, structure et ultrastructure de la branchie d'un Mytilidae des sites hydrothermaux du pacifique oriental. Oceanol Acta 1984; 7:517–23.